Elastic wave propagation in propane gas hydrates

B.I. PANDIT

Department of Geological Sciences, University of Saskatchewan, Saskatoon, Saskatchewan, Canada S7N 0W0

AND

M.S. KING

Earth Sciences Division, Lawrence Berkeley Laboratory, University of California, Berkeley, CA 94720, USA

Compressional (*P*) and shear (*S*) wave velocities of propane gas hydrates and ice were measured as a function of temperature and axial stress. The temperature range extended from − 16.5 to + 2.4°C, and the axial stress varied from 0.53 to 2.1 MPa. Below 0°C, the temperature dependence of both compressional and shear wave velocities was weak; the respective values being 3.25 and 1.65 km/s for propane hydrate and 3.86 and 2.04 km/s for ice. No significant variation of velocity with axial stress was observed below 0°C. Fourier analysis of the signal waveforms through the specimens seems to suggest that the attenuation in hydrates may be greater than in ice.

On a mesuré les vitesses de propagation des ondes de compression (*P*) et de cisaillement (*S*) dans les hydrates de propane et dans la glace, en fonction de la température et des contraintes axiales. La gamme de températures allait de − 16,5 à + 2,4°C, et celle des contraintes axiales de 0,53 à 2,1 MPa. Au-dessous de 0°C, la relation entre la température et les ondes de compression et de cisaillement était mal définie, les valeurs respectives étant 3,25 et 1,65 km/s pour les hydrates de propane et 3,86 et 2,04 km/s pour la glace. Au-dessous de 0°C, on n'a pas observé de variation notable de la vitesse en fonction de la contrainte axiale. L'analyse de Fourier des formes d'ondes des signaux à travers les échantillons semble suggérer que dans les hydrates, l'atténuation des ondes peut être plus forte que dans la glace.

Proc. 4th Can. Permafrost Conf. (1982)

Introduction

Under suitable pressure and temperature conditions, guest molecules of natural gas can fit within the voids in the lattice structure of water molecules acting as the host. Such solid compounds are termed gas hydrates and resemble ice or wet snow. Two environments where hydrate forming conditions are known to exist include the Arctic regions of North America and the Soviet Union, and the sediments below the ocean floor (Bily and Dyck 1974; Cherskii and Makogan 1970; Davidson *et al.* 1978; Judge 1982; Stoll *et al.* 1971). In the Arctic regions, gas hydrate occurrences are associated with relatively thick permafrost sections. Detection of *in situ* gas hydrates is important for two reasons: first, for safe drilling operations during oil exploration in the Arctic, and secondly, as a potential source of hydrocarbons themselves. If seismic methods are to be successfully used not only in detecting gas hydrates but also in distinguishing them from ice, it is necessary to know their seismic wave velocities. Except for the velocity measurements reported by Stoll and Bryan (1979), no velocity data on gas hydrates are available. Furthermore, the measurements by Stoll and Bryan were carried out on a mixture of hydrate (propane) and water. Since then, Whalley (1980) has theoretically derived the ratio of the compressional wave velocities of gas hydrates and ice.

Results are presented here of measurements of compressional (*P*) and shear (*S*) wave velocities of propane gas hydrates and ice, respectively.

Choice of Hydrate

From the point of view of field application, velocity data on methane gas hydrate would be most desirable. The decision to perform measurements on propane gas hydrates instead was based on the following experimental limitation. The hydrate specimen is prepared in one pressure cell but the velocity measurements are carried out in a different cell. This means that during specimen assembly for velocity studies, the hydrate specimen is exposed to atmospheric pressure. From the phase diagram for propane hydrate (Figure 1), it is clear that a temperature–pressure region (A) exists within which the hydrate is stable at atmospheric pressure; hence, the present study was confined to propane hydrates only.

Preparation of Hydrate Specimens

The pressure cell in which the hydrate specimens are prepared (Figure 2) consists of a plexiglass cylinder bounded by brass plates at the top and bottom. Distilled water and propane gas are introduced through an opening in the top brass plate.

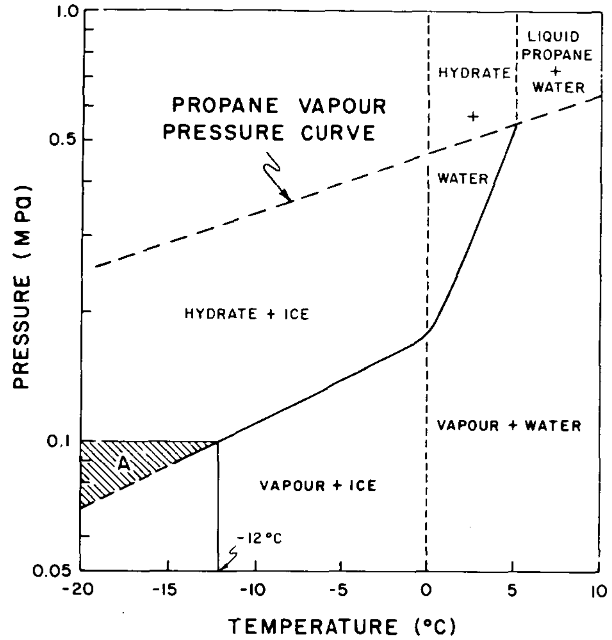

FIGURE 1. Phase diagram for propane hydrate.

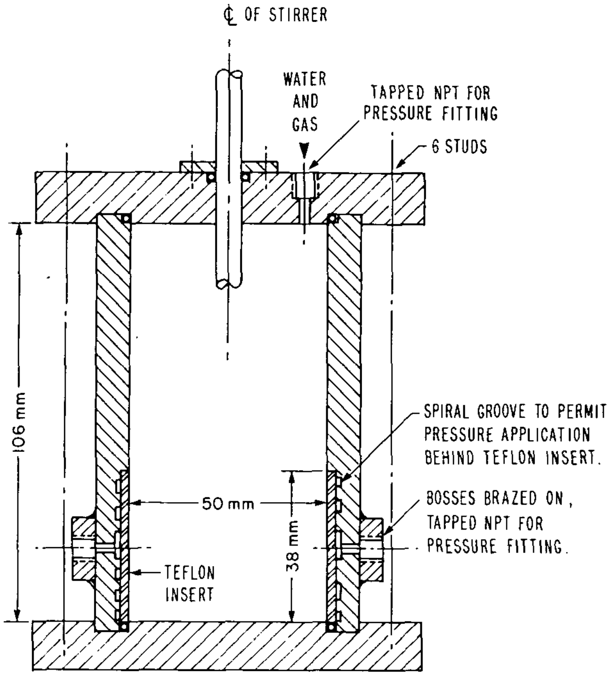

FIGURE 2. Pressure cell for hydrate preparation.

The purpose of the spiral groove behind the teflon insert was to aid in specimen recovery. It was planned to circulate pressurized gas through the groove thus compressing the hydrate specimen sufficiently so that it could be pushed out of the cell easily after the bottom plate was removed. This approach was not followed, however. Instead, the inner surface of the teflon insert was coated with a thin layer of RTV 910 lubricant before introduction of water or gas. The procedure was successful in recovering the hydrate specimen.

The complete apparatus used in hydrate preparation is shown in the schematic diagram (Figure 3). The procedure adopted was as follows:

(i) The temperature of the preparation room was lowered to approximately 2°C;

(ii) The pressure cell was then evacuated;

(iii) Distilled water at about 2°C was then introduced in the cell; and

(iv) Propane gas was added to it at a pressure of 0.4 MPa.

The pressure and temperature conditions in the cell are adequate for forming a hydrate. In fact, a layer of hydrate slurry was observed floating over the water layer. However, it was not possible to produce sufficient quantity of hydrate to prepare a bulk specimen needed to perform velocity measurements.

To prepare bulk specimens used in this study, the procedure followed by Stoll and Bryan (1979) was adopted. Essentially, it consists of mixing liquid propane and water to prepare large quantities of hydrate. Consequently, after addition of the propane gas, as indicated in step (iv), a pressure intensifier was used to liquefy the gas present in the cell. On stirring, a hydrate slurry was formed immediately. Repeated cycles of addition of gas and its subsequent liquefaction enabled the preparation of bulk specimens of propane hydrate.

In order to prepare pure specimens of propane hydrate, the volume of liquid propane should bear a certain ratio to the volume of water in the cell. Taking the molecular formula for propane hydrate to be $C_3H_8.17\ H_2O$, and the density of liquid propane at

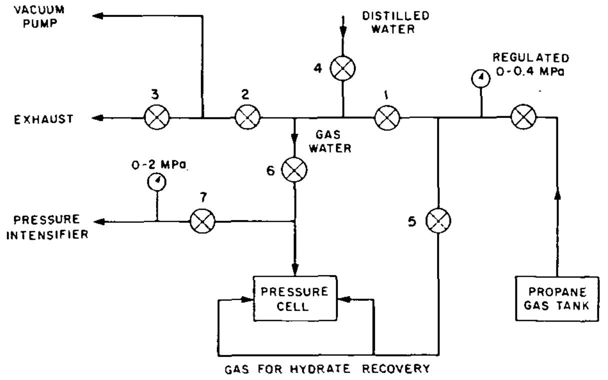

FIGURE 3. Schematic diagram of the complete apparatus.

2°C as 530 kg/m³, it can be shown easily that the volume of liquid propane should be 0.27 times the volume of water. In practice, it is difficult to achieve this ratio exactly; one of the components is very likely to be in excess. The two hydrate specimens involved in the present study had a water (or ice) content in excess of the above formula.

Once the hydrate slurry had been formed, it was left undisturbed for about 24 hours. The slurry then formed a fairly coherent mass. The temperature of the cell was reduced to approximately −18°C, and was maintained so for at least 12 hours. The cell was then disassembled, and the hydrate specimen was pushed out. It was then machined, keeping it at a temperature of −18°C, to produce parallel flat surfaces. The final dimensions and masses of the two hydrate specimens as well as for an ice specimen are given in Table 1. The ice content of the hydrate specimens are qualitative estimates based on the liquid propane/water ratio in the preparation cell.

Some general comments on the hydrate specimens are appropriate here. First, if the liquid propane/water ratio was in excess of 0.27, the resulting hydrate was snow-like in appearance, highly porous, and had a density around 450 kg/m³. Conversely, if the above ratio was less than 0.27, the hydrate specimen was ice-like, compact, and with a density around 800 kg/m³. At this stage, no explanation can be offered to account for these differences. Secondly, no attempt was made to determine if pockets of liquid propane or water were present in the hydrate specimens. Thirdly, the size of the crystals comprising the hydrates also was not determined.

TABLE 1. Physical properties of specimens

	Hydrate I	Hydrate II	Ice
Length (mm)	35.82	25.40	35.31
Diameter (mm)	49.81	49.94	49.15
Density (kg/m³)	850	750	920
Purity	10-20% ice content	5% content	pure

Velocity Measurements

The specimen was first mounted between piezoelectric transducer holders. It was then surrounded by double jackets of tightly fitting thin rubber, over which overlapping vinyl tape was wrapped. This ensured that the DC 200 silicone fluid exerting the confining pressure did not invade the specimen.

A block diagram of the ultrasonic velocity apparatus is shown in Figure 4. The piezoelectric transducer holders are designed to measure compressional (*P*) and shear (*S*) wave velocities sequentially on the same specimen, and are similar to those described by King (1970). The specimen is surrounded in the tri-

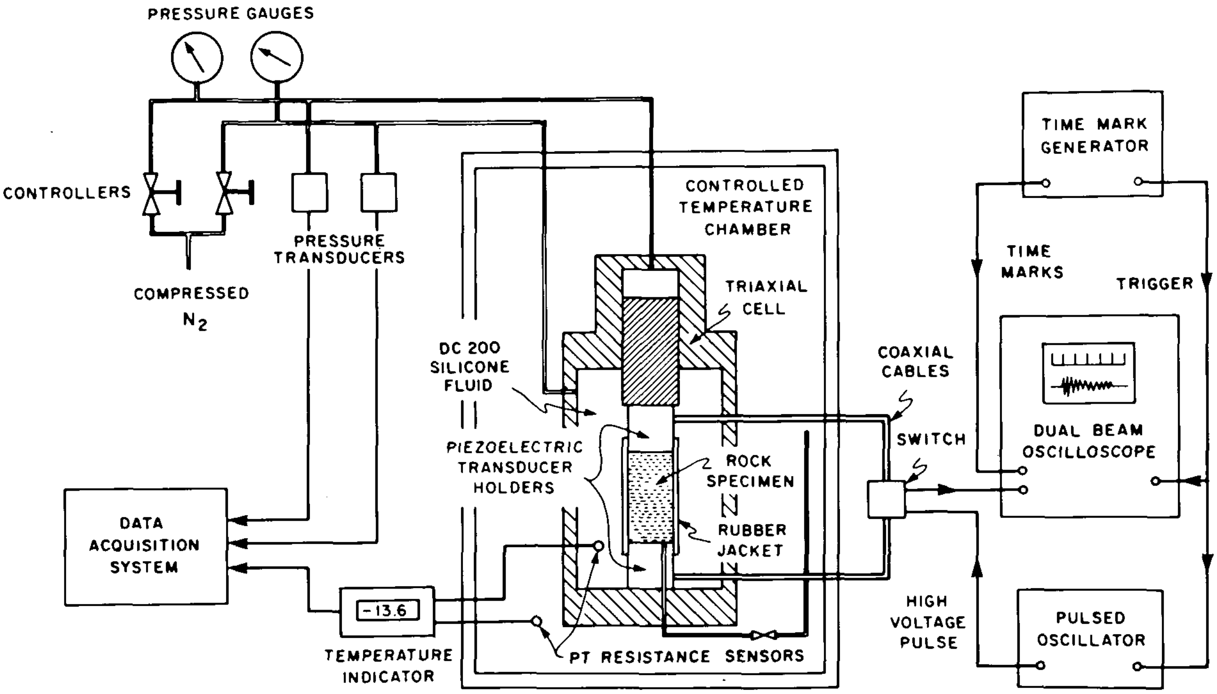

FIGURE 4. Block diagram of ultrasonic velocity apparatus.

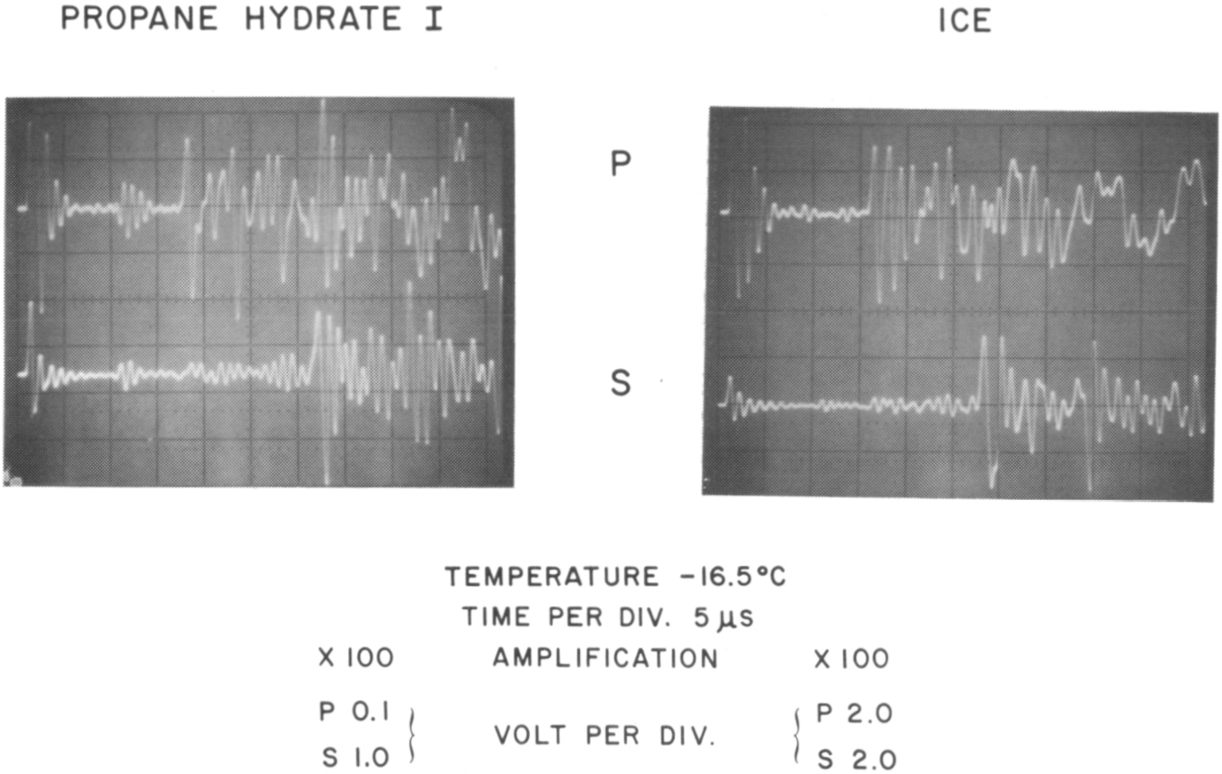

FIGURE 5. Compressional (*P*) and shear (*S*) wave signals through hydrate.

axial cell by DC 200 silicone fluid. Compressed nitrogen is employed to pressurize the DC 200 silicone fluid applying the confining pressure and to apply the axial stress on the specimens. Velocity measurements were made by measuring the time of propagation of a sinusoidally decaying pulse at 820 kHz through the specimen. Velocities were generally measured with an accuracy of ± 1 per cent. Temperatures of the specimens were measured by platinum resistance sensors placed in the triaxial cell close to the specimens.

The confining pressure was maintained at 0.35 MPa throughout the course of the measurements. At any given temperature, the axial stress was varied from 0.53 to 2.1 MPa in two steps. The temperature range over which the velocities were measured extended from −16.5 to +2.4°C. About 24 hours were allowed for the specimens to reach thermal equilibrium.

Results and Discussion

Typical compressional (*P*) and shear (*S*) wave signals through the specimens, namely, propane hydrate I and ice, are shown for successively higher temperatures (Figures 5 to 8). The time of travel through the specimen for either *P*- or *S*-wave is the time corresponding to the arrows shown, minus the travel time for the respective waves when the transducers are in face-to-face contact. As is evident from these figures, *P*-wave arrival times can be determined with great precision throughout the temperature range covered in this study. This is not so for the *S*-wave, especially at temperatures close to 0°C. The *P*-wave signal for 'ice' at 0.2°C corresponds almost to the travel time for transducers when they are in face-to-face contact indicating that the specimen has melted. Also, there is no *S* wave propagating through the specimen any more.

The hydrate specimen at −0.1°C shows a marked increased in *P*-wave travel time; however, the specimen still retains its coherence. This is so even at 2.4°C (*see* Figure 8). It is very difficult to determine the travel time for the *S* wave in these two cases.

The variation of the compressional- and shear-wave velocities is shown as a function of temperature and at an axial stress of 0.53 MPa (Figures 9 and 10). The variation of velocities with axial stress noted in this study was within the error of measurement.

Hydrate I shows insignificant variation with temperature for both velocities as long as the temperature is below 0°C. Above 0°C, a marked drop in the velocities was observed. This drop may be explained

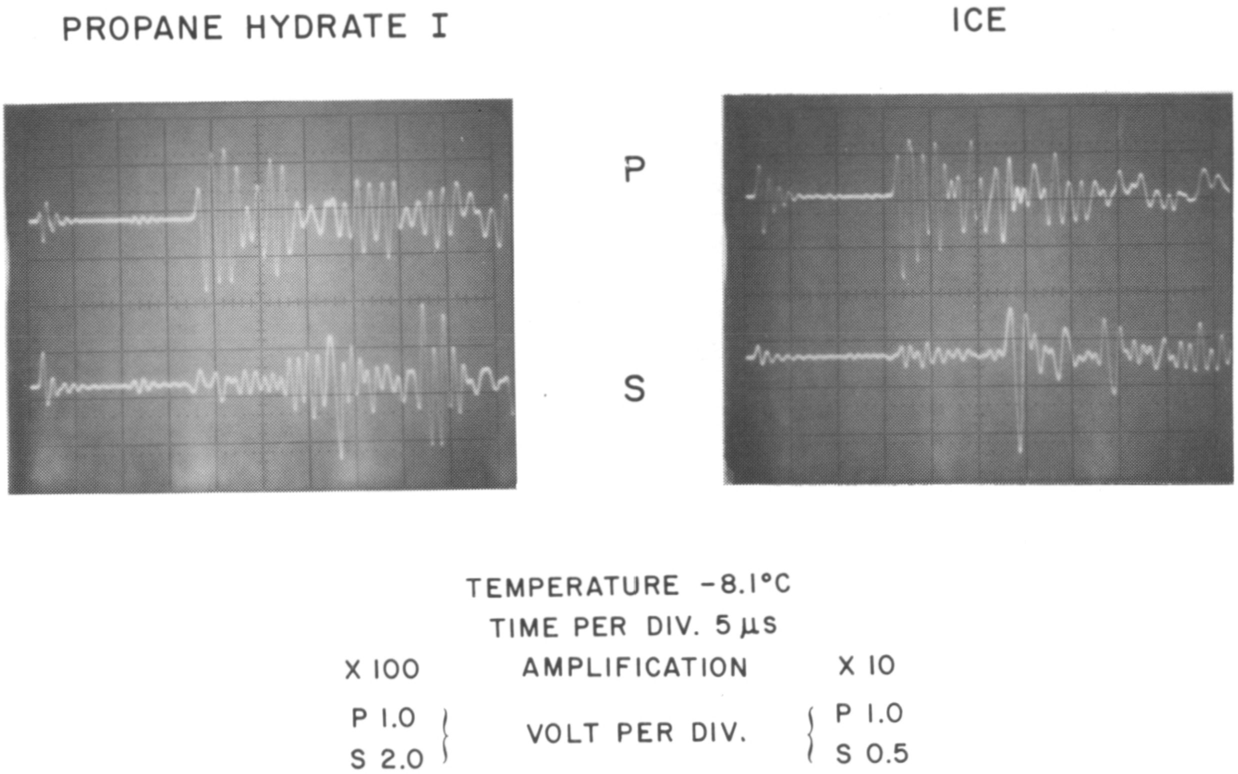

FIGURE 6. Compressional (*P*) and shear (*S*) wave signals through hydrate and ice.

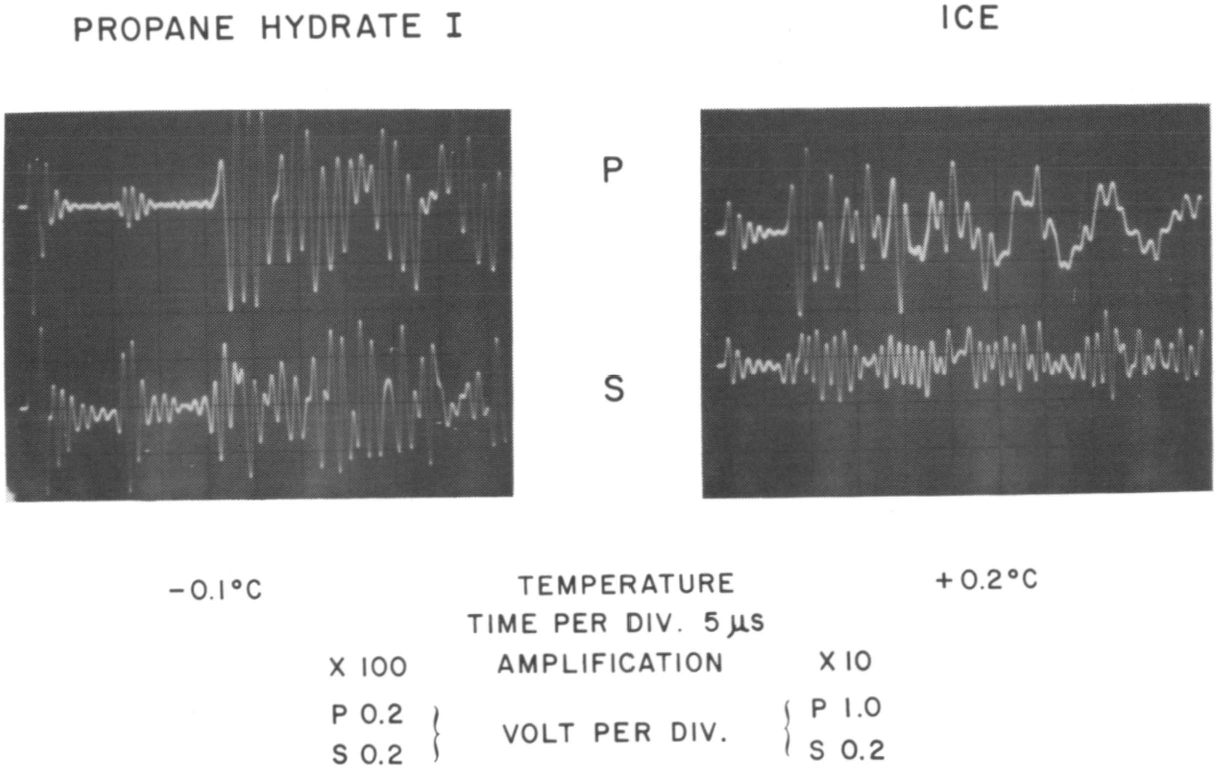

FIGURE 7. Compressional (*P*) and shear (*S*) wave signals through hydrate and ice.

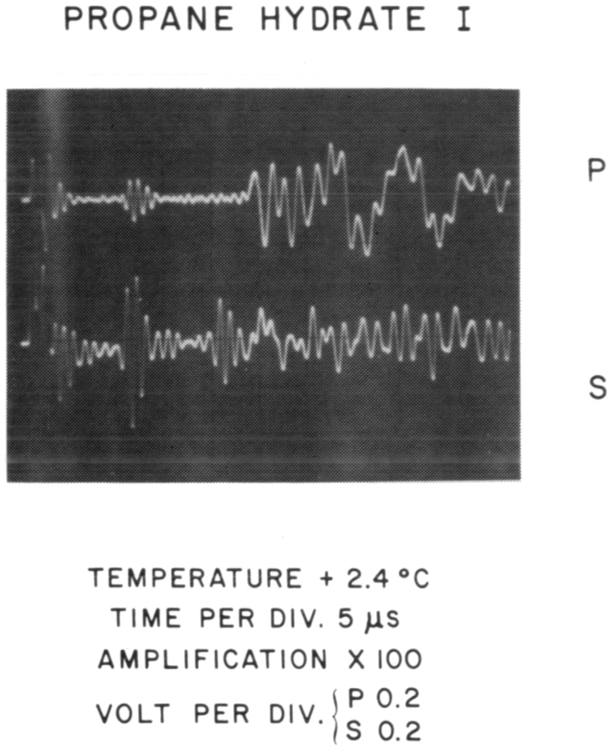

FIGURE 8. Compressional (P) and shear (S) wave signals through hydrate.

due to the melting of the excess ice (10 to 20 per cent) within the specimen. It is worth noting here that on lowering the temperature of the hydrate once again to − 17.4°C, the compressional and shear-wave velocities rose to 3.38 and 2.03 km/s, respectively. Initially, at − 16.5°C, the respective values were 3.24 and 1.65 km/s. The increase in velocity on recycling of temperature may be due to either a shortening of the specimen once its temperature exceeded 0°C or possibly an inherent hysteresis effect. On recovery, the specimen had, indeed, undergone a 0.69-mm reduction in length. Such a small reduction supports the conclusion that the hydrate I was definitely stable and coherent above 0°C. The increase in velocity, therefore, might be due to hysteresis.

The velocity measurements on propane hydrate II had to be abandoned at temperatures above − 5°C due to refrigeration failure in the room in which the velocity cells were kept. The slight increase in velocities for this and the ice specimen are most likely due to compaction. The values of bulk modulus (K), shear modulus (μ) and V_P/V_S ratio for hydrate I and ice specimens at (i) − 16.5°C and (ii) − 1.1°C respectively are given in Table 2.

From theoretical considerations, Whalley (1980) has shown that the compressional-wave velocity for a propane gas hydrate should be 0.945 times the velocity of ice. The corresponding value, as determined in this study, varies from 0.85 at − 16.5°C to 0.82 at − 1.1°C.

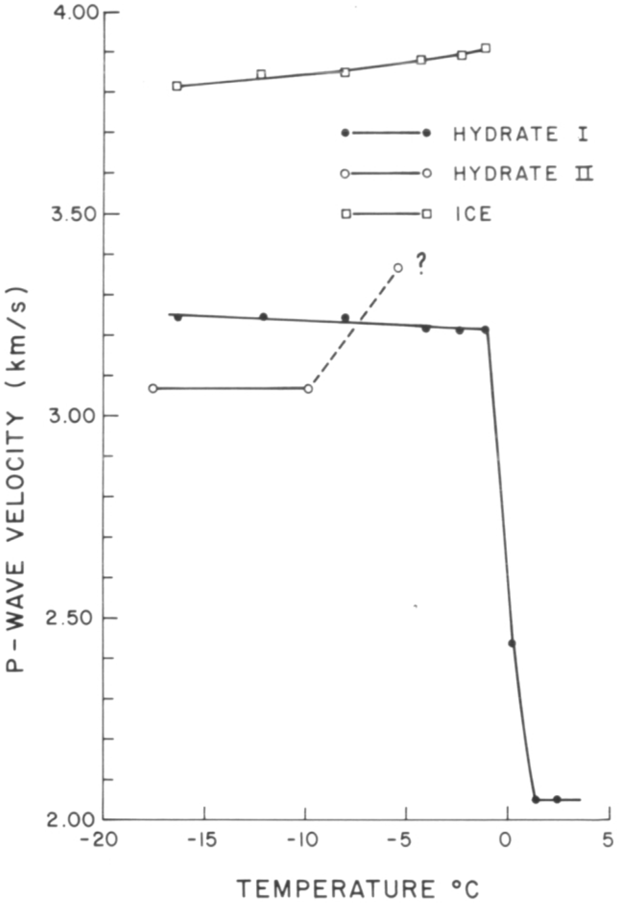

FIGURE 9. Variation of compressional (P) wave velocity with temperature. Axial stress: 0.53 MPa.

The discrepancy between the theoretical and measured values may be due to a number of factors. On the one hand, Whalley's derivation makes a set of assumptions which, if modified, will obviously alter his value of 0.945. On the other hand, the presence of any pockets of liquid propane within the hydrate will cause a reduction in its velocity. Also, at this stage,

TABLE 2. 'K', 'μ' and V_P/V_S for hydrate and ice specimens

Specimen		K (GPa)	μ (GPa)	V_P/V_S
Hydrate I	(i)	5.8	2.3	1.96
	(ii)	5.6	2.4	1.95
Ice	(i)	8.3	3.9	1.87
	(ii)	8.8	3.9	1.88

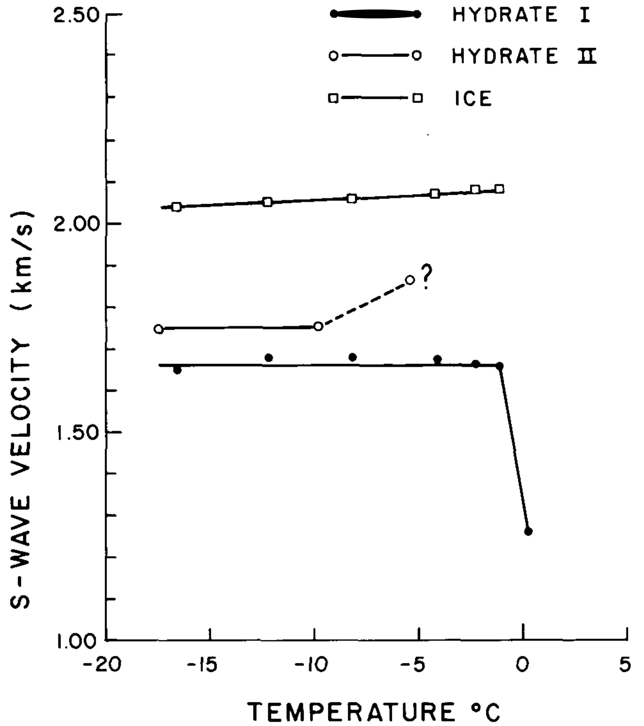

FIGURE 10. Variation of shear (S) wave velocity with temperature. Axial stress: 0.53 MPa.

the variation of velocity with frequency and grain-size is not known for gas hydrates.

It is also of interest to compare the relative attenuation of elastic waves in hydrates and ice specimens. The present study does not allow the determination of the absolute values of intrinsic attenuation for either specimens. Even a comparison of attenuation values is subject to the criticism that the two specimens may possess quite different micro-structures. Despite the above limitations, it is tempting to obtain some estimate — however crude — of the relative attenuation in the two materials; especially, in view of the fact that the dimensions of the hydrate I and ice specimen are very close to one another.

The procedure adopted to acquire some information on the relative attenuation is as follows.

If $E(\omega)$ represents the amplitude spectrum of the received signal when the transmitting and receiving transducers are in face-to-face contact, then

$$E(\omega) = g(\omega)A(\omega)B(\omega) \quad \text{where}$$

$g(\omega)$ represents the amplitude spectrum of the signal input to the transmitting transducer, $A(\omega)$ represents the frequency response function of the transmitting transducer, and $B(\omega)$ represents the frequency response function of the receiver transducer. If $E^1(\omega)$ represents the amplitude spectrum of the received signal when a specimen is placed between the two transducers, then

$$E^1(\omega) = g(\omega)A(\omega)S(\omega)B(\omega) = S(\omega)E(\omega) \quad \text{where}$$

$S(\omega)$ is the response function of the specimen.

$$\therefore \frac{S(\omega)_{\text{Hydrate}}}{S(\omega)_{\text{Ice}}} = \frac{E^1(\omega)_{\text{Hydrate}}}{E^1(\omega)_{\text{Hydrate}}} \div \frac{E^1(\omega)_{\text{Ice}}}{E^1(\omega)_{\text{Ice}}}.$$

The four quantities on the right hand side can be determined by Fourier analysis of the respective signal wave forms. This was done for four values of temperature and the results are tabulated (Table 3). The reason for reporting the values only at the above frequencies lies in the fact that the signal energy of the input is essentially confined within this frequency range, with a peak around 800 kHz. It is clear from Table 3 that the attenuation in the hydrate studied is greater than in ice, however, more precise measurements are needed before this conclusion can be confirmed.

TABLE 3. $S(\omega)_H/S(\omega)_I$ as a function of temperature and frequency

Frequency MHz	Temperature °C -12.1	-8.1	-4.1	-2.3
0.500	0.4	0.3	0.4	0.5
0.625	0.8	1.0	1.0	1.0
0.750	0.8	0.8	0.8	0.8
0.875	0.4	0.1	0.2	0.3
1.000	0.1	0.2	0.2	0.2

Acknowledgements

The present study was performed on a research contract awarded by the Earth Physics Branch, Department of Energy, Mines, and Resources, Ottawa. The authors are very grateful to Dr. A. S. Judge of the Earth Physics Branch for his continued advice and encouragement on gas-hydrate research.

References

BILY, C. AND DICK, J.W.L. 1974. Naturally occurring gas hydrates in the Mackenzie Delta. N.W.T. Bull. of Can. Pet. Geol. vol. 22(3), pp. 340-352.

CHERSKII, N. AND MAKOGAN, Y. 1970. Solid gas - World reserves are enormous. Oil and Gas International, vol. 10(8), pp. 82-84.

DAVIDSON, D.W., EL-DEFRAWY, M.K., FUGLEM, M.O., AND JUDGE, A.S. 1978. Natural gas hydrates in Northern Canada. *In:* Proc. 3rd Int. Conf. Permafrost, vol. 1, Natl. Res. Counc. Can., pp. 938-943.

JUDGE, A.S. 1982. Natural gas hydrates in Northern Canada. *In:* Proc. 4th Can. Permafrost Conf. Calgary, Alberta, 1981, pp. 320-328.

KING, M.S. 1970. Static and dynamic elastic moduli of rocks under pressure. *In:* Rock Mechanics: theory and practice. (ed. W.H. Somerton). Amer. Inst. Min., Metall. and Pet. Eng., New York, NY, pp. 329-351.

STOLL, R.D., EWING, J., AND BRYAN, G.M. 1971. Anomalous wave velocities in sediments containing gas hydrates. J. Geophys. Res. vol. 76, pp. 2090–2094.

STOLL, R.D. AND BRYAN, G.M. 1979. Physical properties of sediments containing gas hydrates. J. Geophys. Res. vol. 84, no. B4, pp. 1629–1634.

WHALLEY, E. 1980. Speed of longitudinal sound in clathrate hydrates. J. Geophys. Res. vol. 85, no. B5, pp. 2539-2542.